Molecular and Crystal Structure of 9-[α-(9*H*-Fluoren-9-ylidene)-4-chlorobenzyl]-9*H*-fluoren-9-yl; an Organic Antiferromagnet with T_N = 3.25 K

Nagao Azuma,*[a] Takehiro Ozawa[a] and Jun Yamauchi[b]
[a] *Department of Chemistry, Faculty of General Education, Ehime University, Matsuyama 790, Japan*
[b] *Graduate School of Human and Environmental Studies, Kyoto University, Kyoto 606, Japan*

The crystal structure of the title radical has been determined by X-ray diffraction at ambient temperature. The crystal system is monoclinic with a space group of *Cc*: a = 33.204(4), b = 9.391(1), c = 15.290(1) Å, β = 101.223(7)°, Z = 8. The final R factor is 0.035 for 2623 observed reflections. There are two crystallographically independent molecules constituting a pair of atropisomers. Two fluoren-9-yl groups and a chlorophenyl moiety are arranged in a propeller shape. The range of the torsion angles of the fluorenyl blades is 25° ~ 33°, and that of the chlorophenyl blades is 55° ~ 59°. The electron-spin exchange pathways are discussed based on the McConnell's spin-density Hamiltonian. The exchange-coupled neighbours are estimated to be z = 6, to which the highest T_N among organic radicals can be attributed.

The title compound is a derivative of the Koelsch radical **1a**. The crystal structures of two complexes of **1a** with benzene and acetone (**1a**·C_6H_6 and **1a**·Me_2CO) are isomorphic.[1a] We have

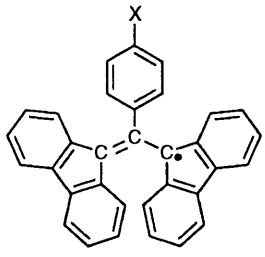

1a X = H
b X = Cl

been concerned about the magnetostructural correlations of the neutral organic radicals with an unpaired electron delocalized over the entire molecular framework such as **1a** and verdazyl radicals.[1b] The magnetic properties of the neutral radicals are characterized by the one-dimensional magnetic chain with an isotropic exchange interaction, that is, the Heisenberg linear chain (hereinafter linear chain). 9-[α-(9*H*-Fluoren-9-ylidene)-4-chlorobenzyl]-9*H*-fluoren-9-yl (**1b**), showed a broad maximum in the magnetic-susceptibility curve at 5.6 K, from which the exchange parameter of J/k = −4.4 K was estimated for the antiferromagnetic linear chain.[2] The same value has been observed for **1a**·C_6H_6.[2]

Most organic radicals show no magnetic phase transition down to the lowest temperature reached with ordinary ^{4}He-cryostats. However, **1b** undergoes a phase transition from a paramagnetic phase to an antiferromagnetic state at the Néel temperature (T_N) of 3.25 K, which belongs to the highest category for T_N amongst the organic radicals,[3a] while T_N of **1a**·C_6H_6 is 1.695 K.[3b] The phase transition can be ascribed to the appreciable exchange interactions among the magnetic chains, since the three-dimensional exchange interactions are necessary for the transition in the spin system with the Heisenberg-type isotropic exchange interaction, as is well known theoretically. Actually, Yamauchi and Deguchi have estimated $|J'/J|$ to be 0.2 for **1b** and only 0.04 for **1a**·C_6H_6, where J' is an interchain exchange parameter.[4] The former ratio is surprisingly large for the π-radicals, because the unpaired electron occupies the p_π-orbitals which are uniaxially perpendicular to the (local) molecular plane. Furthermore, the magnetic heat capacity of **1b** showed that the T_N increased linearly with the hydrostatic pressure to which the radical was subjected, and reached 5.03 K at 5.4 kbar.†[5] The magnetic torque measurements in the antiferromagnetic phase revealed that the easy axis was along the b-axis, and that the anistropy energy was very small.[6] The crystallographic studies of **1b** will provide the fundamental data for understanding these observations and forthcoming findings in the solid state physics and chemistry of **1b**. Therefore, single-crystal X-ray diffractometry has been undertaken at ambient temperature. The electron-spin exchange pathways in this crystal are discussed based on the molecular packing and the calculated spin densities.

† 1 kbar = 10^8 Pa.

Experimental

Materials.—Compound **1b** was prepared according to the procedure reported by Kuhn and Neugebauer.[7] The crystals used for the diffraction were obtained by the careful recrystallization from a mixture of benzene and light petroleum (b.p. 50 ~ 80 °C) at room temp. The crystals obtained from several solutions (benzene–light petroleum, diethyl ether, and acetone) were of hexagonal prisms with the long edge parallel to the c-axis. The Weissenberg photographs showed that they twinned parallel to the A face. The halves were single crystals of suitable quality for diffraction.

Crystal Data.—$C_{33}H_{20}Cl$, M = 451.97. Monoclinic, a = 33.204(4), b = 9.391(1), c = 15.290(1) Å, β = 101.223(7)°, V = 4677(2) Å^3, (by least-squares refinement on diffractometer angles for 25 automatically centred reflections in the range 53.3° ≤ 2θ ≤ 55.0°, 298 K, Cu-Kα radiation, λ = 1.5418 Å), space group *Cc* (No. 9), Z = 8, D_x = 1.284 g cm^{-3}, F(000) = 1880. Blackish crystals. Crystal dimensions 0.45 × 0.25 × 0.18 mm, μ(Cu-Kα) = 15.77 cm^{-1}.

Data Collection and Processing.—Rigaku AFC5R diffractometer, 298 K. Reflections with 4.7° ≤ 2θ ≤ 123.0° were measured with graphite monochromatized Cu-Kα radiation from a fine-focus anode of 12 kW-type rotating-anode generator. The ω-2θ scan mode with a scan rate 16° min^{-1} (in ω) was applied for 3966 reflections (0 ≤ h ≤ 38, 0 ≤ k ≤ 11, −17 ≤ l ≤ 17), 3887 unique (merging R = 0.052

Table 1 Selected bond distances (l), bond angles (φ), and torsion angles (τ) with esds in parentheses

Moledule **A**		Molecule **B**	
	l/Å		l/Å
C(1)–C(2)	1.405(6)	C(41)–C(42)	1.422(6)
C(2)–C(3)	1.413(7)	C(42)–C(43)	1.399(7)
C(2)–C(28)	1.495(7)	C(42)–C(68)	1.506(7)
C(1)–C(5)	1.471(7)	C(41)–C(45)	1.454(6)
C(1)–C(11)	1.456(7)	C(41)–C(51)	1.452(6)
C(4)–C(10)	1.453(7)	C(44)–C(50)	1.459(7)
C(3)–C(17)	1.471(6)	C(43)–C(57)	1.483(7)
C(3)–C(23)	1.465(7)	C(43)–C(63)	1.464(7)
C(16)–C(22)	1.467(7)	C(56)–C(62)	1.453(8)
Cl(1)–C(31)	1.742(6)	Cl(2)–C(71)	1.740(6)
	φ(°)		φ(°)
C(2)–C(1)–C(5)	126.3(5)	C(42)–C(41)–C(45)	125.2(5)
C(2)–C(1)–C(11)	127.4(5)	C(42)–C(41)–C(51)	127.8(4)
C(5)–C(1)–C(11)	106.2(4)	C(45)–C(41)–C(51)	106.7(4)
C(1)–C(2)–C(3)	125.6(5)	C(41)–C(42)–C(43)	125.7(5)
C(1)–C(2)–C(28)	116.1(5)	C(41)–C(42)–C(68)	116.8(4)
C(3)–C(2)–C(28)	118.2(4)	C(43)–C(42)–C(68)	117.5(4)
C(2)–C(3)–C(17)	126.9(5)	C(42)–C(43)–C(57)	125.7(5)
C(2)–C(3)–C(23)	127.0(5)	C(42)–C(43)–C(63)	128.6(5)
C(17)–C(3)–C(23)	105.9(4)	C(57)–C(43)–C(63)	105.5(5)
	τ(°)		τ(°)
C(3)–C(2)–C(1)–C(5)	−151.5(5)	C(43)–C(42)–C(41)–C(45)	151.2(5)
C(3)–C(2)–C(1)–C(11)	31.7(8)	C(43)–C(42)–C(41)–C(51)	−36.6(8)
C(1)–C(2)–C(3)–C(17)	−154.0(5)	C(41)–C(42)–C(43)–C(57)	157.6(5)
C(1)–C(2)–C(3)–C(23)	32.5(8)	C(41)–C(42)–C(43)–C(63)	−27.3(8)
C(1)–C(2)–C(28)–C(29)	57.2(7)	C(41)–C(42)–C(68)–C(69)	−55.6(6)
C(1)–C(2)–C(28)–C(33)	−119.4(5)	C(41)–C(42)–C(68)–C(73)	126.0(5)

after absorption correction), giving 2623 with $I \geqslant 3.00\ \sigma(I)$ which were labelled, observed, and used in the structure refinement. Two rescans were applied for weak reflections. The scan width was $\Delta\omega = (1.63 + 0.30 \tan \theta)°$. Corrections were made for the Lorentz and polarization factors. Three standard reflections monitored at every 150 reflections showed only statistical changes in intensity ($\leqslant 0.5\%$ intensity loss). Semi-empirical correction for absorption was made based on the azimuthal (ψ) scans for five selected reflections.[8] The transmission factors were 0.90 ~ 1.00.

Because the acentric space group of *Cc* suggested by the $N(z)$ test was contradictory to *C2/c* in ref. 6, we examined whether the crystal point group was *m* or *2/m* with the anomalous dispersion due to the chlorine atom. The former point group was supported, and the *Cc* space group was specified.

Structural Analysis and Refinement.—The structure was solved by the direct methods using MITHRIL program.[9] The coordinates and the anisotropic thermal parameters for the non-hydrogen atoms were refined by a full-matrix least-squares procedure based on F with weight $w = 1/\sigma^2(F_o)$. The positions of the hydrogen atoms were idealized (C–H 0.95 Å), assigned isotropic thermal parameters $B(\mathrm{H}) = 1.2\ B_{eq}(\mathrm{C})$, and allowed to ride on their parent carbons. The secondary extinction (coefficient = 4.89×10^{-7}) and the anomalous dispersion were considered in the final stage of the refinement. At convergence, $R = 0.035$, $R_w = 0.036$, S (goodness-of-fit) = 1.48, reflection/parameter ratio = 4.29, max-shift/error ratio = 0.00, and residual electron density = −0.16 ~ 0.14 e Å^{-3}. All calculations were carried out on a VAXstation 3200 with the TEXSAN programs,[10] which used the atomic scattering factors (f, $\Delta f'$, and $\Delta f''$) taken from ref. 11. The relevant tables have been deposited at the Cambridge Crystallographic Data Centre (CCDC).* All measurements and calculations were made at the Advanced Instrumentation Center for Chemical Analysis, Ehime University.

Results and Discussion

There are two crystallographically independent molecules **A** and **B** which constitute an enantiomeric pair. The molecular structures of **A** and **B** are similar to those observed for **1a** in **1a**·C_6H_6 and **1a**·Me_2CO.[1a] Selected bond distances, bond angles and torsion angles appear in Table 1. The atomic deviations of C(2), C(5), C(11), C(17), C(23), C(31) and Cl(1) from the plane defined by C(1), C(3) and C(28) in **A** are −0.027, 0.543, −0.555, −0.538, 0.681, 0.217 and 0.352 Å, respectively; their estimated standard deviations (esds) are 0.005 ~ 0.006 Å. The corresponding deviations in **B** are −0.011, −0.582, 0.705, 0.449, −0.502, 0.143 and 0.261 Å. Comparing the deviations of C(2) and C(42) (see caption of Fig. 1), **A** is inferior to **B** in the planarity around the central carbon atom on the internal allylic chain. The deviations of C(2) and C(31) are twice and three-fold larger than those observed in **1a**.

Molecules **A** and **B** have a similar propeller shape to **1a**, which indicates the atropisomerism due to the bulky fluorenyl blades. The torsion angles of the fluorenyl blades in **A** are 30.1° and 29.3°. In view of the planar arrangement of C(1), C(3), and C(28), this molecule can be regarded as having C_2 symmetry. However, the symmetry of **B** is C_1, for the corresponding angles in **B** are 32.7° and 24.9°. The dihedal angles between two fluorenyl blades in **A** and **B** are about 55°. The torsion angles of the chlorophenyl blades are 58.9° and 54.8° for **A** and **B**, respectively, which are somewhat larger than those observed

* For details of the CCDC deposition scheme, see 'Instructions for Authors', *J. Chem. Soc., Perkin Trans. 2*, 1994, issue 1.

for **1a** (51° and 52°). The fluorenyl groups are puckered into a chair form. In every fluorenyl group, the phenylene planes bend up- and down-ward from the internal cyclopentadiene plane by 1° ~ 5°, respectively, so as to reduce the repulsion between the blades, like those in **1a**.

As shown in Fig. 2(*b*), there are apparently two kinds of the molecular layers parallel to the (100) plane with the separation of about *a*/4 between them; one consists of **A**, the other of **B**. However, the shortest intermolecular contacts are not in these layers. The twinning plane proved to be parallel to the layer.

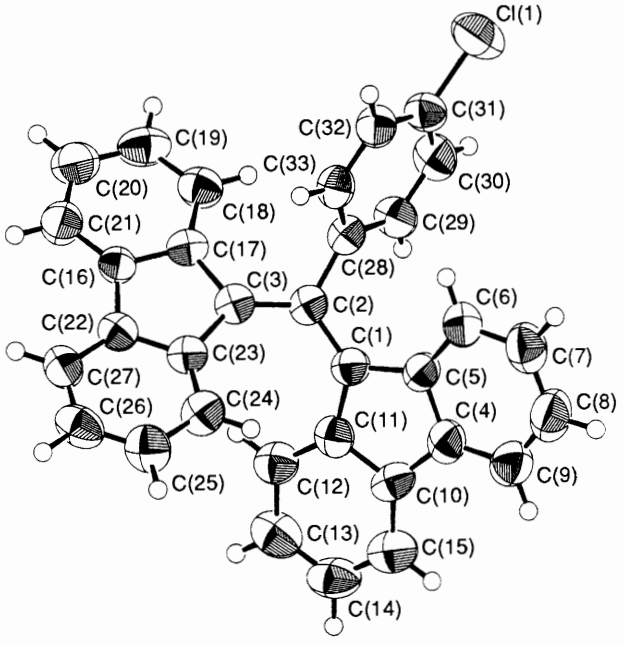

Fig. 1 ORTEP drawing of **A** molecule in the **1b** crystal and the atomic numbering. Ellipsoids are drawn to enclose 50% occupancy. The atomic numbering for **B** molecule is such that the chlorine atom is represented by Cl(2), and the carbon atoms by C(n + 40) where n is the labelling number for the corresponding carbon atom in **A**.

In order to compare **1b** with **1a** in the light of the magnetostructural correlations, we have carried out the same procedure as that applied to **1a**·C_6H_6.[1a] The summation of the triple products in the following McConnell's spin-density Hamiltonian[12] has been applied to the molecular packing [eqn. (1)]; where $\boldsymbol{S}^1$ ($\boldsymbol{S}^2$) is the total spin on molecule **1** (**2**), and ${\rho^1}_i$

$$H^{12} = -\boldsymbol{S}^1 \cdot \boldsymbol{S}^2 \sum {J^{12}}_{ij} {\rho^1}_i {\rho^2}_j, \qquad (1)$$

(${\rho^2}_j$) is the π-spin density on the i (j)-th atom in molecule **1** (**2**). The spin densities on **1b** were admitted to be the same as those calculated for **1a**,[1a] because of the similar molecular structure, and because of the small change in the spin-density distribution by the perturbation of the chlorine substituent on the phenyl ring which lies on the nodal plane. Approximating the exchange integral ${J^{12}}_{ij}$ with the direct proportion to the σ-overlap integral[13] between the relevant p-orbitals, the summation in eqn. (1) has been applied in turn to intermolecular contacts shorter than 4.0, 4.5 and 5.0 Å, and the results are shown in Table 2. The positive sum should indicate an antiferromagnetic exchange interaction in the present approximation.

The sums in Table 2 can be divided into two classes; one is almost independent of the limitation in the interatomic distances, the other is otherwise. If all spin densities were positive, the sums would increase with the increase in the limiting distance. Therefore, the presence of the convergent sums may be a distinctive feature of the system with negative spin densities.

Two pairs of the first- and second-largest sums indicate antiferromagnetic linear chains along two different directions;

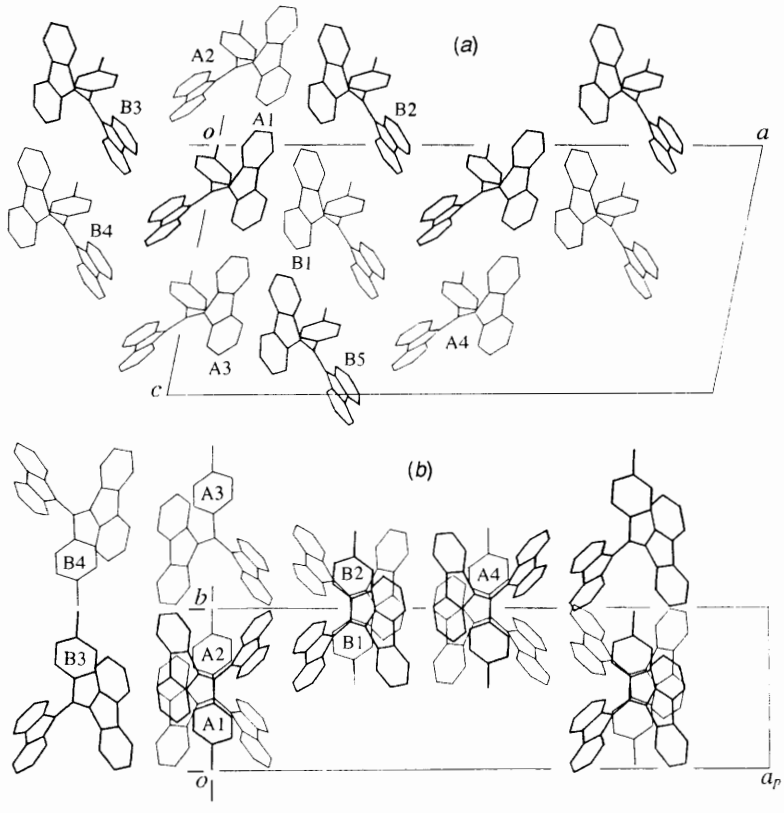

Fig. 2 Molecular packing in the **1b** crystal viewed along the *b*-axis (*a*), and along the *c*-axis (*b*). The symbol a_p represents the *a*-axis projected on the plane perpendicular to the *c*-axis. The symbols A*n* and B*n*, A and B of which designate **A** and **B** molecules in the **1b** crystal, are used in Table 2 and in the text in order to specify the positions in the lattice.

Table 2 Pertinent intermolecular contacts (l) in the **1b** crystal[a] and sums of the triple products in eqn. (1)

Atom	Atom	ADC[b]	l/Å	Atom	Atom	ADC	l/Å
Between A1 and B3 (n-glide-reflected **B1** at $b = 3/4$)[c]							
C(16)	C(48)	I	3.830	C(16)	C(49)	I	3.852
C(17)	C(49)		3.971	C(22)	C(48)		3.588
C(23)	C(48)		3.986	C(27)	C(48)		3.696
C(32)	C(55)		3.670				
Sum of the triple products: 7.55, 14.6, 14.2[d]							
Between A1 and **B2** (c-glide-reflected **B1** at $b = 1$)							
C(7)	C(66)	II	3.703	C(8)	C(64)	II	3.965
C(8)	C(65)		3.423	C(8)	C(66)		3.407
C(8)	C(67)		3.923				
Sum of the triple products: 9.81, 10.5, 10.9							
Between A1 and A2 (c-glide-reflected A1 at $b = 1/2$)							
C(16)	C(32)	III	3.743	C(18)	C(6)	III	3.739
C(18)	C(7)		3.684	C(20)	C(33)		3.995
C(21)	C(32)		3.749	C(21)	C(33)		3.655
C(22)	C(32)		3.755	C(27)	C(32)		3.875
Sum of the triple products: 5.10, 1.47, 7.87							
Between B1 and B2 (c-glide-reflected B1 at $b = 1$)							
C(58)	C(46)	II	3.691	C(58)	C(47)	II	3.865
C(59)	C(46)		3.703	C(69)	C(44)		3.979
C(69)	C(48)		3.793	C(69)	C(49)		3.542
C(70)	C(44)		3.637	C(70)	C(49)		3.576
C(70)	C(50)		3.780	C(70)	C(55)		3.928
Sum of the triple products: 4.57, 4.20, 6.60							
Between B1 and B5 (B2 translated ***b*** and ***c***)							
C(65)	C(60)	IV	3.713	C(65)	C(61)	IV	3.798
C(66)	C(60)		3.695				
Sum of the triple products: 4.25, 4.21, 3.90							
Between A1 and A3 (c-glide-reflected A1 at $b = 1$)							
C(13)	C(8)	V	3.939	C(13)	C(9)	V	3.968
C(14)	C(8)		3.895				
Sum of the triple products: 2.87, 2.80, 2.67							
Between A1 and B1 translated $-\boldsymbol{b}$							
C(29)	C(67)	VI	3.983	C(30)	C(61)	VI	3.958
Sum of the triple products: 0.008 74, 1.89, 6.67							
Between A1 and B1 (within asymmetric unit)							
C(15)	C(56)	VII	3.926	C(15)	C(57)	VII	3.860
C(15)	C(73)		3.696				
Sum of the triple products: −0.0274, 7.32, 7.57							
Between B1 and A3 (c-glide-reflected A1 at $b = 1$)							
The same results as those between A1 and B2 are obtained, because of the c-glide reflection.							
Between B1 and A4 (n-glide-reflected A1 at $b = 3/4$)							
The same results as those between A1 and B3 are obtained, because of the n-glide-reflection.							

[a] Estimated standard deviations are 0.005–0.01 Å. [b] Roman numerals in ADC column refer to the following equivalent positions of the latter atoms relative to the deposited atomic coordinates. The coordinates of the former atoms are those deposited. (I) $-1/2 + x, 3/2 - y, -1/2 + z$; (II) $x, 2 - y, -1/2 + z$; (III) $x, 1 - y, 1/2 + z$; (IV) $x, 3 - y, 1/2 + z$; (V) $x, 2 - y, 1/2 + z$; (VI) $x, -1 + y, z$; (VII) x, y, z. [c] A1,A2,....,B1,B2.... indicate the molecules specified in Fig. 2. [d] The values were obtained for the limitation $d \leqslant 4.0$, 4.5 and 5.0 Å, respectively, where d was the interatomic distance used in the calculation for the sum of the triple products in eqn. (1). The unit of the value is in 10^{-5}.

one has a molecular sequence of the B3===A1---B2 repeating units along the $(1\bar{1}0)$ plane, the other has a series of the A3---B1===A4 units along the (110) plane, as shown in Fig. 2. In this Figure, the molecules providing these sequences are distinguished with the thick and fine lines. The molecular arrangements in these sequences are undoubtedly alternating, which causes the magnetic alternating linear chains. These chains do not intersect, but pass each other spatially; at every passing point two alternating chains are coupled through the A1 · · · A2 or **B1** · · · B2 exchange interaction. These two sums provide their respective antiferromagnetic linear chains along the c-axis. Both A1 · · · A3 and B1 · · · B5 couplings are also antiferromagnetic but weaker than the last two. Thus, the number of interacting neighbours of $z = 6$ is suggested for both **A** and **B**, which is consistent with the unique magnetic character of **1b** represented by the highest T_N of those of neutral organic radicals.

The maximum sum calculated for the antiferromagnetic linear chain in the **1a**·C_6H_6 crystal is similar to that of **1b**,[1a] which is in good accord with the fact that the same J parameter has been observed for both **1a**·C_6H_6 and **1b**. True, the respective sums (antiferromagnetic) calculated for the **1a** pairs—the molecules in every pair belonged to neighbouring magnetic chains—were as large as the intrachain one, but they were, altogether, cancelled into a small effective exchange interaction among the chains. This cancellation (frustration) was ascribed to the characteristic molecular packing. On the other hand, such cancellation has not been found in the **1b** crystal. The existence of the cancellation is probably responsible for some of the differences between the magnetic properties of the two radicals. An established example for the cancellation has been found in K_2NiF_4, the two-dimensional antiferromagnetic interaction of which has been explained by the cancellation between the neighbouring layers.[14]

Indeed the magnetic susceptibility as well as the heat capacity of **1b** were explained by the Heisenberg linear chain model,[2,3a] but this explanation has not been established as yet, because the maximum susceptibility showed significant downward deviation from the theoretical value, despite the high temperature susceptibility indicated 100% in radical concentration.[2] This discrepancy could be improved with the alternating chain model.[15] Two- or three-dimensional effects may be also responsible for the discrepancy.

The shortest C · · · C contacts of all are observed between the A1---B2 couple with 3.41(1) and 3.423(9) Å which are very close to the van der Waals diameter of the carbon atom (3.40 Å), while the shortest C · · · C contact in the A1===B3 couple is 3.588(7) Å. These values symbolize the alternation in the exchange interaction. In order to obtain a good understanding of the magnetic properties, it is interesting to know whether the linear dependence of T_N on the hydrostatic pressure can be correlated dominantly with the reduction in the interatomic distances, or correlated significantly with the distortion in the molecular structure followed by the improvement on the above inhomogeneity. Recalling the degrees of freedom of the torsion angles and the puckering angles mentioned earlier, the onset of similar structural changes may be observed by the diffraction studies for the crystal chilled deeply from room temperature. The X-ray and neutron diffractometries at far low temperature and at high pressure are worthy of note in this sense and in the spin structure of **1b**.

Acknowledgements

We wish to thank Professor S. Tomiyoshi of Ehime University for valuable discussions.

References

1 (*a*) N. Azuma, T. Ozawa and J. Yamauchi, *Bull. Chem. Soc. Jpn.*, 1994, **67**, in the press; (*b*) N. Azuma, J. Yamauchi, K. Mukai, H. Ohya-Nishiguchi and Y. Deguchi, *Bull. Chem. Soc. Jpn.*, 1973, **46**, 2728; N. Azuma, Y. Deguchi, F. Marumo and Y. Saito, *Bull. Chem. Soc. Jpn.*, 1975, **48**, 819; 1975, **48**, 825; N. Azuma, *Bull. Chem. Soc.*

Jpn., 1980, **53**, 2671; 1982, **55**, 1357; N. Azuma, K. Tsutsui, Y. Miura and T. Higuchi, *Bull. Chem. Soc. Jpn.*, 1981, **54**, 3274.
2 J. Yamauchi, *Bull. Chem. Soc. Jpn.*, 1971, **44**, 2301.
3 (*a*) J. Yamauchi, K. Adachi and Y. Deguchi, *J. Phys. Soc. Jpn.*, 1973, **35**, 443; J. Yamauchi, *J. Chem. Phys.*, 1977, **67**, 2850; (*b*) W. Duffy, Jr., J. F. Dubach, P. A. Pianetta, J. F. Deck, D. L. Strandburg and A. R. Miedema, *J. Chem. Phys.*, 1972, **56**, 2555.
4 J. Yamauchi and Y. Deguchi, *Bull. Chem. Soc. Jpn.*, 1977, **50**, 2803.
5 (*a*) J. Yamauchi, K. Takeda and M. Inoue, *Chem. Lett.*, 1990, 1551; J. Yamauchi, K. Takeda and M. Inoue, *Mol. Cryst. Liq. Cryst.*, in the press.
6 H. Ozaki, H. Ohya-Nishiguchi and J. Yamauchi, *Phys. Lett.*, 1975, **54A**, 227. The space group of $C2/c$ designated in this reference is error; it should be Cc. The conclusions in the paper are not affected by this change.
7 R. Kuhn and F. A. Neugebauer, *Monatsh. Chem.*, 1964, **95**, 3.
8 A. C. T. North, D. C. Phillips and F. S. Mathews, *Acta Crystallogr., Sect. A*, 1968, **24**, 351.
9 G. J. Gilmore, *J. Appl. Crystallogr.*, 1984, **17**, 42.
10 TEXSAN, Texray Structure Analysis Package, version 5.0, Molecular Structure Cooperation, The Woodlands, TX 77381, 1989.
11 *International Tables for X-Ray Crystallography*, D. Reidel Pub. Co., Dordrecht, The Netherlands, 1985, vol. III, p. 276.
12 H. M. McConnell, *J. Chem. Phys.*, 1963, **39**, 1910.
13 The program for the overlap integral between Slater 2p-orbitals appears in O. Kikuchi, *Bunshikidoho*, Kodansya, Tokyo, 1980, p. 137.
14 M. E. Lines, *Phys. Rev.*, 1967, **164**, 736; R. J. Birgeneau, H. J. Guggenheim and G. Shirane, *Phys. Rev. Lett.*, 1969, **22**, 720; L. J. de Jongh and A. R. Miedema, *Adv. Phys.*, 1974, **23**, 1.
15 J. C. Bonner, H. W. J. Blote, J. W. Bray and I. S. Jacobs, *J. Appl. Phys.*, 1979, **50**, 1810.

Paper 3/05108K
Received 24*th August* 1993
Accepted 18*th October* 1993